Available online at www.sciencedirect.com
SCIENCE DIRECT®
Journal of Chromatography A, 1083 (2005) 14–22
JOURNAL OF CHROMATOGRAPHY A
www.elsevier.com/locate/chroma

Comprehensive pore structure characterization of silica monoliths with controlled mesopore size and macropore size by nitrogen sorption, mercury porosimetry, transmission electron microscopy and inverse size exclusion chromatography

Dieter Lubda [a,*], Wolfgang Lindner [b], Milene Quaglia [c], Cedric du Fresne von Hohenesche [c], Klaus K. Unger [c]

[a] *Merck KGaA, LSP R&D MDA, Frankfurter Str. 250, 64271 Darmstadt, Germany*
[b] *Institute of Analytical Chemistry, University of Vienna, Währinger Str. 38, A-1090 Vienna, Austria*
[c] *Institute of Inorganic Chemistry and Analytical Chemistry, University of Mainz, Duesbergweg 10-14 D-55099 Mainz, Germany*

Received 20 July 2004; received in revised form 3 May 2005; accepted 19 May 2005

Abstract

The porosity of monolithic silica columns is measured by using different analytical methods. Two sets of monoliths were prepared with a given mesopore diameter of 10 and 25 nm, respectively and with gradated macropore diameters between 1.8 and 7.5 μm. After preparing the two sets of monolithic silica columns with different macro- and mesopores the internal, external and total porosity of these columns are determined by inverse size-exclusion chromatography (ISEC) using polystyrene samples of narrow molecular size distribution and known average molecular weight. The ISEC data from the 4.6 mm analytical monolithic silica columns are used to determine the structural properties of monolithic silica capillaries (100 μm I.D.) prepared as a third set of samples. The ISEC results illustrate a multimodal mesopore structure (mesopores are pores with stagnant zones) of the monoliths. It is found by ISEC that the ratio of the different types of pores is dependent on the change in diameter of the macropores (serve as flow-through pores). The porosity data achieved from the mercury penetration measurement and nitrogen adsorption as well of scanning electron microscopy (SEM) and transmission electron microscopy (TEM) pictures are correlated with the results we calculated from the ISEC measurements. The ISEC results, namely the multimodal pore structure of the monoliths, reported in several publications, are not confirmed analyzing the pore structures of the different silica monoliths using all other analytical methods.

Keywords: Monolithic silica; Inverse size-exclusion chromatography; Mercury penetration; Transmission electron microscopy; Scanning electron microscopy; Nitrogen adsorption

1. Introduction

In recent years, chromatographic support materials of the monolithic type to be classified also as porous continuous beads has gained increasing interest for various reasons. The development of monolithic columns was a breakthrough in the area of fast separation.

Different research groups [1–4] have studied basic developments of monolithic materials for use in separation sciences. Based on the nature of the material from which they are made, monolithic columns can be classified as organic polymer- or silica (inorganic)-based columns. The first monolithic columns prepared as foams were based on organic polymers [5], which were later be adopted to be used as chromatographic columns [6,7] In parallel, Nakanishi and Soga [8] developed a new sol–gel process for the preparation of monolithic silica columns with a bimodal pore structure (i.e. with macropores which serves as flow-through pores

* Corresponding author. Tel.: +49 6151 72 7642; fax: +49 6151 72 917642.
E-mail address: dieter.lubda@merck.de (D. Lubda).

0021-9673/$ – see front matter © 2005 Elsevier B.V. All rights reserved.
doi:10.1016/j.chroma.2005.05.033

and mesopores). The process is based on the hydrolysis and poly-condensation of alkoxysilanes in the presence of water-soluble polymers. Different groups [3,4] demonstrated that this method allows the preparation of analytical chromatographic columns (4.6 mm I.D.) with high efficiencies and low column backpressures.

The concept is also applicable to the generation of monolithic fused silica capillary columns where the porous body is in situ synthesized inside the capillary. The capillaries are applied in *n*-LC and CEC separations [9–11]. The morphology of the adsorbents offers optimum mass transfer properties for HPLC separations of low molecular weight as well as for high molecular weight analytes [12]. The morphology and the pore structure of a chromatographic bead are the most important features in the design of broadly useful HPLC packings, as these aspect directly influence the hydrodynamic properties (e.g. flow properties), thermodynamic properties (e.g. loadability) and the mass transfer kinetics (e.g. efficiency).

The pore structural parameters of monolithic silica prepared as rods can be assessed by traditional methods [13] such as gas sorption [14], mercury intrusion (porosimetry) [15] and transmission electron microscopy. In this case, the SEC [16,17] or inverse size exclusion chromatography (ISEC) can be a method of choice as there exists a correlation between the pore diameter values and the size of the macromolecules to be separated.

Halàsz and Martin [18] used ISEC to determine the PSD of porous materials and numerous studies helped to establish and to summarize the theoretical and methodological background of the technique [19–25]. Examples of characterization of silica [26,27] or polymeric [28–32] stationary phases by ISEC are reported in the literature. In this context Ishizuka et al. [33] investigated the pore structure of monolithic silica capillaries and columns by ISEC. A recent investigation by Guiochon and co-workers [34,35] of the pore structure of such 4.6 mm I.D. monolithic silica columns based on ISEC showed that a large fraction (75–80%) of the total column porosity was due to macropores with pore diameters of 0.3 μm or larger and only a small fraction (3%) of the porosity was contributed by pores whose diameter was in the range between 50 and 300 nm. The porosity due to the mesopores was approx. 10–12%.

The goal of this study was to further investigate the reported ISEC experiments by Guiochon and co-workers [35] for the 4.6 mm I.D. columns and to compare the ISEC data to the results obtained from classical methods such as mercury porosimetry, nitrogen adsorption as well as electron transmission (TEM) and electron scanning microscopy (SEM).

2. Experimental

2.1. Materials and methods

2.1.1. Classification of materials employed in this study

The ISEC experiments were first performed on two sets of Chromolith® monolithic silica columns (Merck KGaA, Darmstadt) having a nominal diameter of 4.6 mm and a length of 10 cm. For “set one” the mesopore diameter was kept constant (approx. 10 nm calculated using mercury porosimetry) and the macropore diameter varied between 1.8 and 7.0 μm. For “set two” the mesopore diameter was found to be approx. 25 nm (according to mercury porosimetry measurements) and the diameter of the macropores varied from 1.9 to 7.5 μm. The monolithic silica columns were cladded with poly-ether-ether-ketone (PEEK) by a proprietary process of Merck KGaA, Darmstadt.

Additionally, a third set of monolithic fused silica capillaries was prepared comparing the properties of these capillaries with those of the 4.6 mm I.D. monolithic columns described above. The 100 μm I.D. capillary columns as well as the 4.6 mm I.D. materials were prepared by exactly the same synthesis protocol described in detail by Motokawa et al. [36]. The preparation of monolithic structures within such capillaries has the substantial practical advantage that no cladding procedure is needed as for the 4.6 mm I.D. columns.

In order to analyze such porous materials the following two types of techniques are generally used: direct and indirect techniques.

Direct techniques provide actual images of the surface but no significant quantitative characterization of the surface area and pore volumes could be obtained. Examples of techniques are microscopy, electron microscopy and X-ray analysis.

Indirect techniques, which measure the macroscopic effects of phenomena occurring in the pore volume and on the pore surface, are gas adsorption and mercury penetration. In addition a chromatographic method, as ISEC, could also be a powerful method to quantitatively characterize the pore morphologies of the monolithic samples prepared for this study.

2.1.2. Inverse size-exclusion chromatography (ISEC)

ISEC on monolithic 4.6 mm I.D. columns was carried out by using an HPLC 1100 (Agilent Technologies, Waldbronn). ISEC experiments were performed with Tetrahydrofuran (THF) as the solvent (HPLC LiChrosolv® grade Merck KGaA; Darmstadt). Monolithic fused silica capillaries were measured by using a split injection HPLC 1100 instrument and an HPCE^{3D} as UV-detector. Polystyrene standards with a molecular weight ranging from 484 to 10,300,000 Da were from Polymer Standards Service, Mainz, Germany, and dissolved in THF at a concentration of 0.1 mg/ml. Benzene was used for the determination of the total accessible porosity of the column. The experiments on the 4.6 mm I.D. monolithic columns were assessed at a flow rate of 1 ml/min, by injecting 1 μl of each standard. The experiments at the capillaries were carried out at a flow rate of approximately 140 nl/min and 1 nl of the polymer solution was injected. UV detection was at 210 nm.

A list of the tested materials in ISEC and of the corresponding pore structural parameters from mercury intrusion measurements as well as results we received from nitrogen adsorption is reported in Table 1.

Table 1
Pore structural parameters measured by mercury penetration and nitrogen adsorption of prepared monolithic silica materials of 4.6 mm I.D.

Lot-No.	Mean macropore diameter (Hg-Poro) [μm]	Mean mesopore diameter (Hg-Poro) [nm]	Mean macropore vol. (Hg-Poro) [ml/g]	Mean mesopore vol. (Hg-Poro) [ml/g]	S_{BET} [m^2/g]
DL02/1.8/120	1.8	10.9	2.55	0.88	298
DL02/1.8/WP	1.9	25.0	2.62	0.85	143
DL03/2.5/120	2.4	10.5	2.54	0.86	309
DL03/2.5/WP	2.5	24.5	2.65	0.85	144
DL04/3.0/120	3.0	10.0	2.50	0.83	313
DL04/3.0/WP	3.0	24.0	2.58	0.85	136
DL05/3.5/120	3.5	10.9	2.61	0.84	299
DL05/3.5/WP	3.4	24.0	2.61	0.83	142
DL06/4.5/120	4.5	10.2	2.50	0.84	283
DL06/4.5/WP	4.5	23.0	2.54	0.81	125
DL07/5.0/120	5.0	10.0	2.52	0.85	311
DL07/5.0/WP	5.3	22.4	2.49	0.82	131
DL08/6.0/120	5.7	10.0	2.46	0.84	310
DL08/6.0/WP	6.0	24.4	2.62	0.85	140
DL09/7.0/120	7.0	10.0	2.60	0.85	313
DL09/7.0/WP	7.5	22.8	2.19	0.79	132

Set 1 = 1.8–7 μm macropores and approx. 10 nm mesopores. Set 2 = 1.9–7.5 μm macropores and approx. 25 nm mesopores.

2.1.3. Mercury penetration

The mercury porosimetry measurements were accomplished with a Pascal 440 (containing a Pascal 140 unit) equipment from CE-INSTRUMENTS (Wigan, UK).

In literature, it was reported [35] that the authors were unable to use mercury porosimetry for the pore structural characterization of silica monoliths, as the monoliths were not compatible with the available instruments and the column tubing could not withstand the required pressure. However, with the sample holder (CE-instruments) used, we were able to measure samples of more then one centimeter. Using such a holder, we could analyze the porosity of segments of several centimeters from the PEEK cladded columns. The mercury was able to penetrate even the smallest macropores (about 1.9 μm in diameter) of the compared silica monoliths using a pressure of lower than 10 bars since the macroporous structure is composed of highly connected throughpores. For an estimation of the corresponding pore diameter from the applied pressure (in bars) we used the Washburn equation with the surface tension of mercury of 480 dynes/cm and a contact angle of mercury on a silica surface of 140°.

2.1.4. Nitrogen adsorption

The nitrogen adsorption measurements were carried out with an ASAP 2400 from Micromeritics (Norcross, USA) at 77 K. This equipment measures automatically the adsorption and desorption isotherms and calculates the BET (BET is the abbreviation of the names Brunauer, Emmett and Teller) surface area as well as the one point surface area, the total volume of mesopores and the mesopore size distribution according to the BJH (BJH is the abbreviation of the names Barrett, Joyner, Halenda) method.

2.1.5. Scanning electron microscopy and transmission electron microscopy

For the scanning electron microscopy we employed a JSM-6300F instrument from JEOL LTD. Tokyo, Japan. To compare data of a direct analytical method to the ISEC results, images were taken using the scanning electron microscopy (SEM). The SEM images in this work were obtained using an operation voltage of 5 KV and emission current of 7–8 μA. For the samples preparation, we deposited a piece of silica monolith onto the Au/Pd (80:20) target. The silica monoliths were sputtered with a 5 nm thick gold layer under vacuum to improve conductivity, using a SCD 040 instrument from Balzers. We prepared images from the different silica monoliths with mesopores of ∼10 and ∼25 nm and macropores between 1.8 and 7.5 μm in order to reconfirm the ISEC results.

The transmission electron microscopy (TEM) images were taken using a CM20 from Philips at an operation voltage of 120 kV. For the measurement of the silica skeleton we crushed the 4.6 mm silica monolithic samples and used the resulting small pieces after depositing the material onto the TEM-grid.

3. Results and discussion

3.1. Sol–gel formation of monolithic silica materials

In order to prepare the different sets of monolithic silica materials we used a sol–gel system starting from a multicomponent solution consisting of silica oligomers with a broad mass distribution, a solvent mixture, and additives according to a standard protocol [36,37]. During spinodal decomposition, a co-continuous (sponge-like) domain structure develops and remains unbroken for a substantial period of time. After increasing the domain size, a fragmentation of the domains results in a continuous matrix. Because macroporous gel domains are formed in the wet stage, further tailoring the internal pore structure by exchanging the fluid phase can be performed more efficiently and in less time than gel

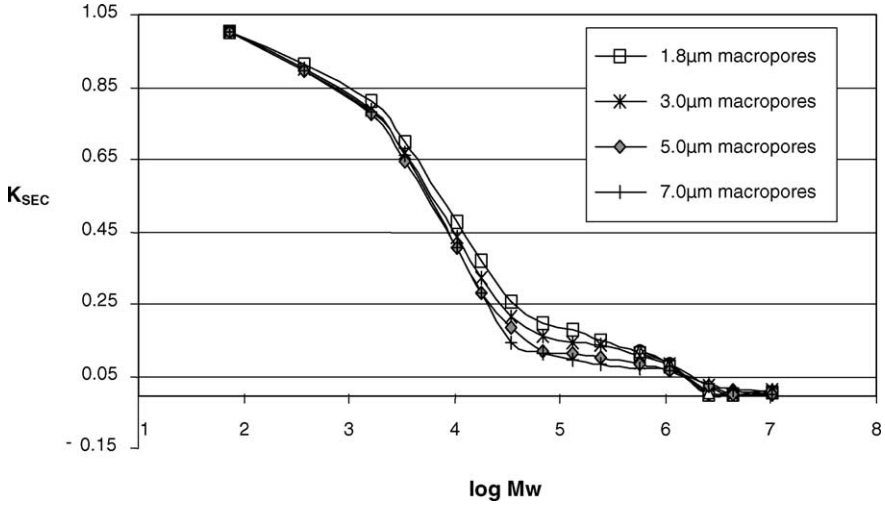

Fig. 1. SEC curves, K_{SEC} plotted against the log of the molecular weight (MW) of the polystyrene standards, calculated on the set 1 of 4.6 mm I.D. monolithic silica materials with four different macropores keeping the mesopores fixed at approx. 10 nm mesopores (conditions see Section 2).

monoliths without macropores [38]. Using that knowledge during the production and independent control of macropore and mesopore sizes, different silica monoliths with narrowly distributed continuous pores in discrete size ranges were fabricated.

3.2. Inverse size-exclusion chromatography

The SEC calibration curves we carried out showed an exclusion limit at 5000 K Da. In Fig. 1, the exclusion curves calculated on the set of columns characterized by ca. 10 nm mesopores (mesopores are pores with stagnant zones) are reported. A similar behavior for the set of columns with ca. 25 nm mesopores and for the capillaries was observed (data not shown). The definition of the exclusion limit appears to be dependent on the macropore (the macropores serve as flow-through pores) dimensions; more specifically it is changing by decreasing the macropore dimensions. The presence of two exclusion limits suggests the existence of a bimodal system within the pore network. In Table 2, the pore size of the two sets of materials (set 1 = 1.8–7 μm macropores and 10 nm mesopores, set 2 = 1.9–7.5 μm macropores and ca. 25 nm mesopores) calculated by ISEC are reported. The dimension of the mesopores, which have to be considered as pores with stagnant zones, found is comparable with the dimensions of the mesopores calculated by mercury intrusion as well as by nitrogen adsorption measurement. The dimension of the calculated macropores varies randomly around 300 nm. The macropores, which serve as flow-through pores, with pore diameter between 1.9 and 7.5 μm cannot be measured by ISEC due to the lack of high molecular weight standards as well as due to the danger of blocking the chromatographic system (thus the monolithic through-pores of the column) during the evaluation.

Table 2
Comparison of pore structural parameters of 4.6 mm I.D. columns with 1.8–7 μm macropores and approx. 10 nm mesopores as well as 1.9–7.5 μm macropores and approx. 25 nm macropores measured by mercury penetration and calculated using ISEC measurements

Lot-No.	Mesopore diameter (Hg-Poro) [nm]	Mesopore diameter ISEC [nm]	Macropore diameter ISEC [nm]
DL02/1.8/120	10.9	17.2	283
DL02/1.8/WP	25.0	36.4	372
DL04/3.0/120	10.0	14.2	327
DL04/3.0/WP	24.0	37.2	352
DL07/5.0/120	10.0	14.2	335
DL07/5.0/WP	22.4	36.4	352
DL09/7.0/120	10.0	14.8	291
DL09/7.0/WP	22.8	36.4	372

In order to estimate the importance of the two fractions of macropores on the total porosity, the elution volume of benzene injected into the monolithic columns was considered representative of the total porosity volume and each elution volume was normalized to this value. In Fig. 2, the elution volume percentage (Ve%) of each polymer under investigation was plotted against the log of the molecular weight (MW) of the polystyrene standards. This normalization was needed in order to better compare the differences between the samples. By considering the elution volume percentages, it was possible to calculate the percentage of the mesopores, of the ca. 300 nm macropores and thus of the nano-porosity, accessible by ISEC, relative to the total porosity of the monolithic columns with different macropore diameter structure. This fact is reflected in Fig. 3 for the columns characterized by ca. 10 nm mesopores. A similar behavior was observed for the columns characterized by mesopores of ca. 25 nm (data not shown). The percentage of mesopores contributing to the total porosity of the monolithic columns is constant and amounts to approx. 25%. The percentage of the 300 nm pores is decreasing with increasing the macropore dimensions covering the range from 3 to 8% of the total porosity.

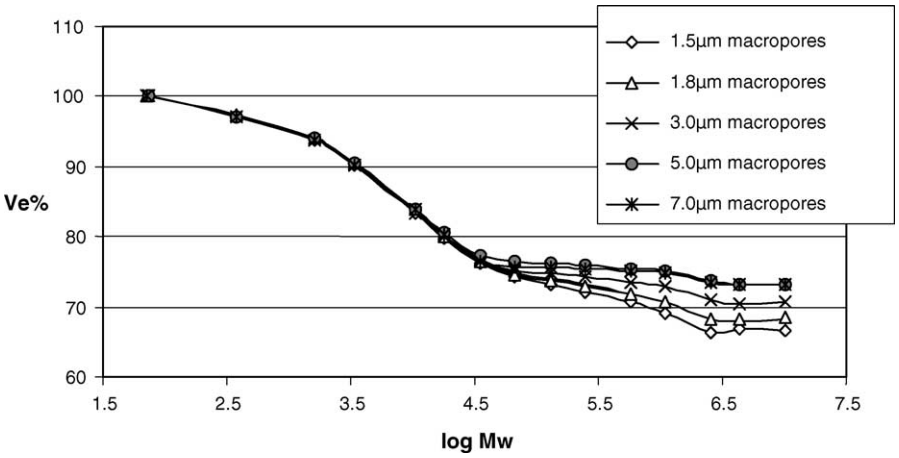

Fig. 2. Elution volume percentage (Ve%) plotted against the log of the molecular weight (MW) of the polystyrene standards, calculated on the set of 4.6 mm I.D. monolithic silica materials with five different macropores characterized by ~10 nm pores.

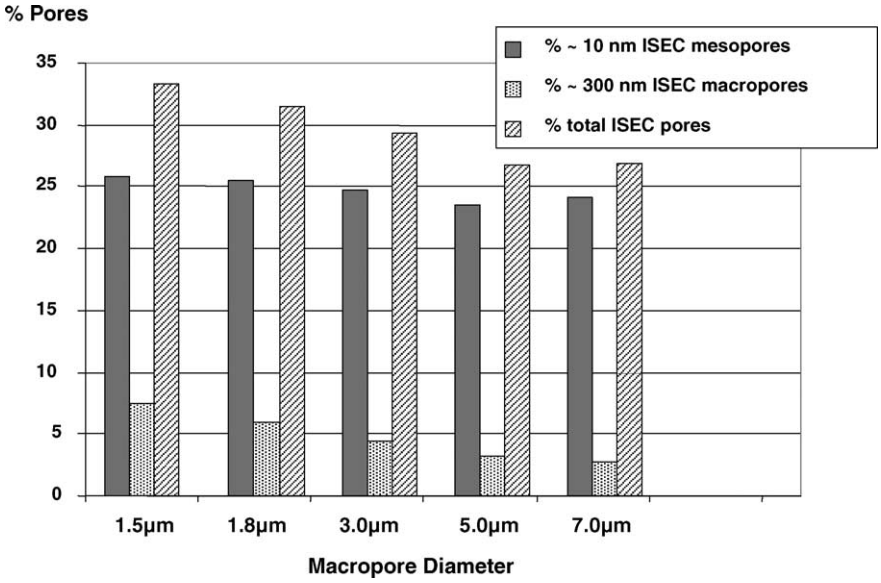

Fig. 3. Percentage of the mesopores and of the 300 nm macropores calculated from the ISEC results on the total measured porosity of the monolithic columns.

In Table 3, the pore size calculated by ISEC of the sets of monolithic materials (100 μm I.D. monolithic silica capillaries as well as 4.6 mm PEEK cladded monolithic silica columns) we prepared using the same preparation procedure is reported. Considering the percentage of the mesopores on the total porosity of capillaries and columns, one can observe a difference of 3–8% of mesopores within the skeleton of the silica inside of the 100 μm I.D. capillaries in comparison with the 4.6 mm I.D. columns. This lack can be probably explained due to a partly incomplete solidification process of the monolithic structure within the capillaries, which is minimal within the 4.6 mm I.D. monolithic columns due to the PEEK cladding process. Even if the observed difference concerning porosity has to be taken into account the ISEC

Table 3
Comparison of pore structural parameters of 4.6 mm I.D. columns and 100 μm I.D. capillaries with different macropores measured by mercury penetration and calculated using ISEC measurements

Lot-No.	Column ID	Mesopore diameter (Hg-Poro) [nm]	Mesopore diameter ISEC [nm]	Macropore diameter ISEC [nm]
DL10/0.5/120	4.6 mm	13.3	14.2	287
DL10/0.5/120	100 μm	–	20.4	277
DL11/1.3/120	4.6 mm	12.0	15.0	294
DL11/1.3/120	100 μm	–	22.6	316
DL12/2.1/120	4.6 mm	10.0	15.4	295
DL12/2.1/120	100 μm	–	15.1	238

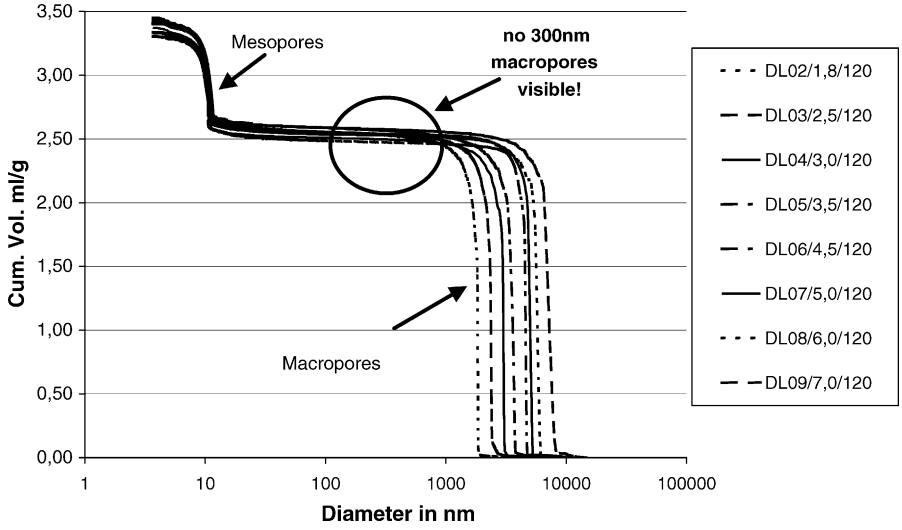

Fig. 4. Determination of eight variations (1.8, 2.5, 3.0, 3.5, 4.5, 5.0, 6.0 and 7.0 μm) of macropores using mercury porosimetry.

gave reproducible results by comparing the method within one preparation batch. As the shrinkage of the monolithic gel, prepared within the capillary tubing, was found to be in the order of the containing macropores it was found to have only a minor influence on the performance of the capillary.

3.3. Mercury porosimetry

Mercury porosimetry is one of the few methods, which is able to detect pore diameters of porous materials from 3.6 nm to 15 μm. As the monolithic silica columns encapsulated within PEEK, can withstand pressures up to 200 bars during the chromatographic separations it should be possible to use the mercury porosimetry for the determination of the macropores of the encapsulated (cladded) silica monoliths. The pressure difference between the outer pressure applied onto the PEEK cover and the pressure at the internal monoliths is relevant for a possible collapse of a column. Due to sufficiently high resistance of the PEEK cladding to the pressure used we were able to even determine the size of the mesopores using mercury penetration measurements. One important reason not to use cladded monoliths for the precise determination using mercury intrusion was the lack of accuracy concerning the real weight of the silica within the PEEK cladded monoliths. Due to the fact that uncladded samples of the prepared silica monoliths were available we preferred to use them for the comparison of porosity measurements.

As can be seen from Fig. 4, the samples of monolithic silica materials prepared with a relative constant mesopore size of about 10 nm but with a variation of macropores from 1.8 to 7.0 μm were measured using uncladded monoliths of 4.6 mm diameter. This indicates that the method of spinodal phase decomposition, which was used for the preparation of the monolithic silica supports, is able to generate structures of different macropores independent from the mesopore size. Moreover, Fig. 4 shows for the variation of mesopores as well of the macropores a relative narrow and similar distribution of the pore diameter. A plateau (which indicates that the sample contains no pores of this corresponding diameter) could be found for all monolithic silica materials in the pore size range between 50 and 1000 nm. Thus no other pores, even in small amounts, were detectable using the mercury porosimetry, as evidenced by ISEC measurements for 300 nm pores.

In other words, with the mercury intrusion method we were not able to correlate the ISEC data, which needs an explanation. On the one hand we have to take into account that the data of the physical properties of mercury found in the literature varies to a large extent. On the other side there is the danger of an influence based on different measuring principles or set-up's using different instruments.

We used the commonly accepted contact angle of 140° and a surface tension of 484 dynes/cm at 25 °C for calculating the pore structural data from mercury porosimetry. As the values of the contact angle and surface tension are very much depending on the nature and surface energy of the sample we determined the contact angle independently by using a video instrumentation and a plain slice of a silica monolith. In order to measure the real contact angle for the given silica monoliths one mercury droplet was deposited onto the plain silica surface and was evaluated from a picture taken from the video camera revealing a contact angle of 141°. In contrast to that result, we found in literature values for contact angle from 125 to 152° for calculations of porous silica materials using mercury penetration.

By taking the same raw data measured, we got for a contact angle of 140° a pore diameter of 2.25 μm and a variation of the pore diameter from 1.79 μm (125°) to 2.65 μm (152°) for the macropores and from 7.5 nm (125°) to 11.9 nm (152°) for the mesopores. In addition the contact angle is a function of temperature and pressure. During the measurement the pressure was raised up to 4000 bars (400 MPa or 58,000 psi). Because the mercury is compressible, the temperature of the sample increased from 22 to 30 °C. The variation of

temperature is nearly independent from the sample because the heat capacity of mercury exceeds that of the silica, but it may influences the measurement of mesopores much more than the macropores. This introduces a systematic error, which we tried to compensate during the mathematical calculation by correcting the obtained results, analyzing the monolithic silica samples, by subtracting the data we got from the measurement of a sampling device filled with pure mercury.

The network of a macropores silica monolith provides a flow path through and along the column for the mercury and ensures access to the whole network of mesopores. Only pores with access to the surface and bigger than 3.5 nm can be filled by using an instrumentation with a pressure limit of 4000 bars, it is evident that any blind or closed pores remain unfilled using mercury intrusion. In order to check whether the monolithic material contains such large pores inside the skeleton, which are blocked by mesopores, we crushed one sample and repeated the mercury intrusion measurement. As expected, in the part of the diagram corresponding to the macropores a lower pore volume and a little broader distribution of macropores were received as we reduced the amount of the macropores during the crushing. In contrast to the macropore volume we got the same diameter and only a little bit lower pore volume for the containing mesopores. We were not able to detect any blind macropores or pores in the range of about 100–1000 nm as reported using the ISEC protocols.

Alié et al. [39] discussed that porosimetry data are affected by isostatic compression of the monolith at pressures up to about 80 MPa (800 bars). Consequently to be able to measure all mesopores larger than 3.5 nm using mercury intrusion measurement, the pressures applied to the monolithic silica materials has to be raised up to 4000 bars. Of course the material has to withstand that pressure. Using the Washburn equation we were able to calculate the corresponding pore diameter, which is reached using a pressure of about 800 bars, to be approximately 10 nm. The pressure, which should be applied to penetrate 300 nm pores with mercury is approx. 50 bars. Verifying the pressure/volume curves during the measurement, that should show compressions or a collapse of the sample, reconfirmed that the mercury penetration result of the measurement could be used for the evaluation of the silica monoliths without restrictions.

3.4. Nitrogen adsorption results

Nitrogen sorption at 77 K is an established technique to assess the specific surface area according to BET [14], the specific pore volume according to the Gurvitsch rule and the pore size distribution according to the BJH method [40].

The nitrogen adsorption is able to detect pore diameters of less than ca. 100 nm diameter using the desorption isotherm to calculate the distributions of the pore size, thus we used the method to confirm the results of the mesopores structure received from the mercury penetration measurement.

It was reported in a publication [35] that the authors were not able to use the nitrogen adsorption measurement as the monoliths have dimensions that are not compatible with those of conventional nitrogen-sorption instrumentations. As Micromeritics offers a holder for larger samples, we were able to circumvent this and to analyze the surface area of parts of several centimeters from the PEEK cladded column. The same reason not to use the cladded monoliths was the lack of accuracy concerning the real weight of the plain silica monoliths inside of the tubing, as it was the same case for the mercury penetration measurement. Thus, we used for all our comparisons a piece of uncladded silica monoliths. As recommended before [41], we used the results of the desorption isotherm, as it corresponds to a lower energy hence a more stable state as the data received by the adsorption isotherm, for the calculation of mesopores of the 4.6 mm I.D. monolithic silica samples. Data of measured surface area of the different materials are summarized in Table 1. The calculated mesopore diameters (data not shown here), which were needed for the comparison with the data obtained with mercury intrusion, confirmed the results we obtained. No other pores larger than 30 nm, thus also no macropores proposed from the ISEC results, could be detected.

3.5. Scanning electron microscopy

We prepared SEM images from the different silica monoliths of mesopores of 10 nm and ca. 25 nm and macropores between 1.8 and 7.5 μm in order to reconfirm the ISEC results.

As depicted in Fig. 5, a relative smooth surface could be observed on the SEM pictures of the silica monoliths, containing different macropore sizes, by using a magnification of 3000. Even with a magnification of more than 50,000 times only a globular kind of surface on the silica skeleton could be observed. No pores in the range of approx. 300 nm, proposed by the ISEC measurements, were detectable. Comparing the surface roughness of silica monoliths with the smaller macropores (1.5–3.5 μm) with the larger ones (>3.5 μm) the obtained pictures showed a little smoother skeleton surface for the larger pores.

3.6. Transmission electron microscopy images

Transmission electron microscopy provides an image of very small structures. In fact, it allows object separation down to the Ångstrom scale. In Fig. 6, two TEM images, one of a silica monolith with mesopores of 10 nm and one with 25 nm are shown. The pictures indicate a homogeneous pore size distribution of the pore within the skeleton without visible mesopores in the area of bigger than 50 nm and again no macropores of approx. 300 nm, calculated from the ISEC measurements, could be observed.

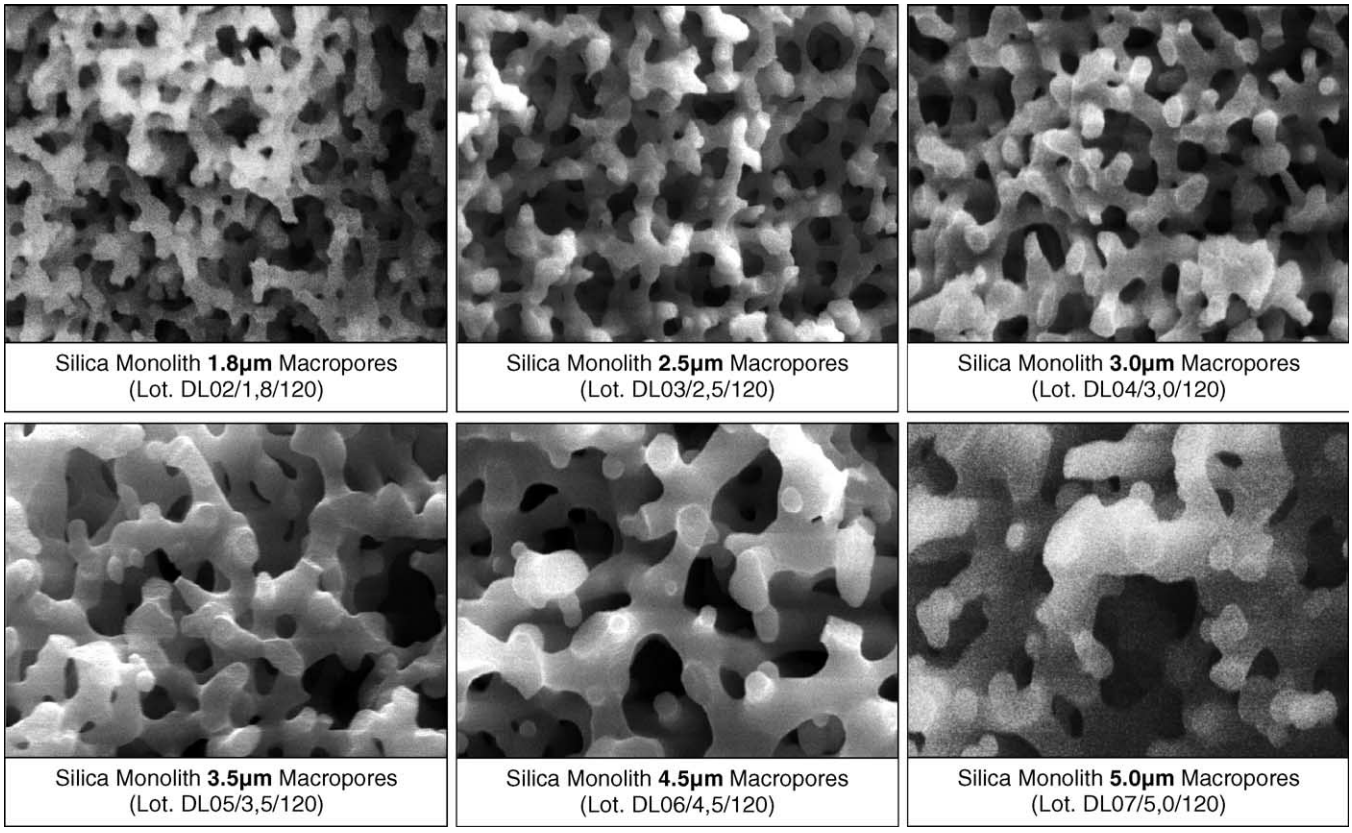

Fig. 5. SEM pictures of the silica monoliths, containing different macropore diameters (diameter specified on the figure) using a magnification of 3000.

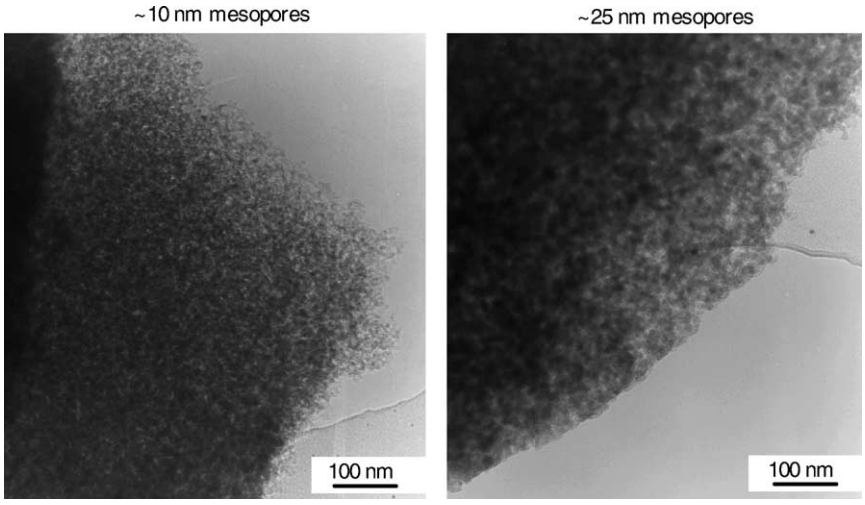

Fig. 6. Two TEM images, one of a silica monolith with mesopores of approx. 10 nm and the other one with pores of approx. 25 nm.

4. Conclusion

Due to our results, the 300 nm macropores reported from other groups [33,35] during the evaluation of standard monoliths, seem to be a kind of artefact or caused by not yet fully understood phenomena effecting the ISEC measurements. As the only chromatographic method the advantage of ISEC is that it is a non-destructive analytical technique to determine the pore structure of a material. A requirement of the ISEC is the need of very well-defined molecular weight and spherically shaped standards that span the dimensions of the pores to probe the accessibility of the pores. Any deviation of the idealized models will lead to divergent results. As ISEC only provides a calculated statistical representation of the pore width that allows the effluent transport, we might need more knowledge about the real behavior of polystyrene standard

molecules, of such a wide ranges of molecular weight (from 484 to 10,300,000 Da), to probe monolithic porous systems. Additionally, it has to be consider at this point also, that macropores are pores with stagnant zones.

We recognized that by analyzing smaller macropore (and skeleton) size monoliths, the "apparent" 300 nm pores increase. Since the building of the skeleton surface is closely related to the interfacial smoothening during the dynamic processes of phase separation and gelation, it seems possible that gels with larger macropores, which serves as flow-through pores, and thicker skeletons have a smoother skeleton surface. One possible explanation is, that the "apparent" pores are a kind of influence of the macroporous system of the monolithic skeleton to the structure of the polystyrene standard molecules during the measurement somewhat related to a deformation from ideally spherical shape.

In contrast no pores within the skeleton in the dimension of 100–300 nm on all the SEM as well as on the TEM pictures, even using high magnification being able to see pores very clearly, could be observed. The same results we got by measuring the containing pores of all monolithic samples we prepared using the mercury intrusion and nitrogen adsorption technique. As a conclusion we have to consider that the observed ISEC results must be regarded as being model-dependent, and it is essential to have this in mind in context with its interpretation. One possible adoption we have to consider for the calculation of ISEC results in the future might be the introduction of a tortuosity factor as it is the case for the characterization non-regularly shaped porous materials including membranes.

Acknowledgements

We would like to thank Dr. Cabrera, Mrs. Czerny and Mr. Friedrich from the analytical group of the analytics and reagents department of Merck KGaA for their help during the preparation and evaluation of the monolithic silica columns. For helpful discussion on the interpretations of the ISEC results, we would further thank Dr. Grimes and Dr. Hennessy from the University of Mainz.

References

[1] Ch.M. Zeug, J.-L. Liao, K. Nakazato, S. Hjerten, J. Chromatogr. A 753 (1997) 227.
[2] S. Xie, F. Svec, J.M.J. Frechet, J. Chromatogr. A 775 (1997) 65.
[3] K. Cabrera, D. Lubda, H.-M. Eggenweiler, H. Minakuchi, K. Nakanishi, J. High Resol. Chromatogr. 23 (2000) 99.
[4] H. Minakuchi, K. Nakanishi, N. Soga, N. Ishizuka, N. Tanaka, Anal. Chem. 68 (1996) 3498.
[5] W.D. Ross, R.T. Jefferson, J. Chromatogr. Sci. 8 (1970) 386.
[6] S. Hjertén, J.L. Liao, R. Zhang, J. Chromatogr. A 473 (1989) 273.
[7] F. Svec, J.M.J. Fréchet, Anal. Chem. 54 (1992) 820.
[8] K. Nakanishi, N. Soga, J. Non-Cryst. Solids 139 (1992), 1–13 and 14–24.
[9] D. Wistuba, V. Schurig, J. Chromatogr. A 875 (2000) 255.
[10] Z. Chen, M. Niitsuma, K. Uchiyama, T. Hobo, J. Chromatogr. A 999 (2003) 75.
[11] B. Barroso, D. Lubda, R. Bischoff, J. Proteome Res. 2 (2003) 633.
[12] K.K. Unger, C. du Fresne, B. Bidlingmaier, M. Gruen, K. Schumacher, R. Ditz, D. Lubda, M. Schulte, K. Nakanishi, N. Ishizuka, A.T. Liapis, B.A. Grimes, COPS VI (2002).
[13] G. Guiochon, M. Sarker, J. Chromatogr. A. 704 (1995) 237.
[14] S. Brunauer, P.H. Emmett, E. Teller, J. Am. Chem. Soc. 60 (1938) 309.
[15] H.L. Ritter, L.C. Drake, Ind. Eng. Chem. 17 (1945) 782.
[16] L.G. Aggebrandt, O. Samuelson, J. Appl. Polym. Sci. 8 (1964) 2801.
[17] J.R. Carmichael, Macromolecules 1 (1968) 526.
[18] I. Halàsz, K. Martin, Angew. Chem. Int. Ed. Engl. 17 (1978) 901.
[19] E.F. Casassa, J. Phys. Chem. 75 (1971) 275.
[20] M.E. Van Kreveld, N. Van Den Hoed, J. Chromatogr. 83 (1973) 111.
[21] J.H. Knox, H.P. Scott, J. Chromatogr. 316 (1984) 311.
[22] J.H. Knox, H.J. Ritchie, J. Chromatogr. 387 (1987) 65.
[23] R.L. Rill, D.H. Van Winkle, B.R. Locke, Anal. Chem. 70 (1998) 2433.
[24] M. Goto, B.J. McCoy, Chem. Eng. Sci. 55 (2000) 723.
[25] N.V. Saritha, G. Madras, Chem. Eng. Sci. 56 (2001) 6511.
[26] A. Kurganov, V. Davankov, T. Isajeva, K. Unger, F. Eisenbeiss, J. Chromatogr. A 660 (1994) 97.
[27] H. Guan, G. Guiochon, J. Chromatogr. A 731 (1996) 27.
[28] M. Zecca, A. Biffis, G. Palma, C. Corvaja, S. Lora, K. Jerabek, B. Corain, Macromolecules 29 (1996) 4655.
[29] E.C. Peters, F. Svec, J.M.J. Fréchet, Chem. Mater. 9 (1997) 1898.
[30] M. Ousalem, X.X. Zhu, J. Hradil, J. Chromatogr. A 903 (2000) 13.
[31] D. Whitney, M. McCoy, N. Gordon, N. Afeyan, J. Chromatogr. A 807 (1998) 165.
[32] S.M. Howdle, K. Jeràbek, V. Leocorbo, P.C. Marr, D.C. Sherrington, Polymer 41 (2000) 7273.
[33] N. Ishizuka, H. Minakuchi, K. Nakanishi, N. Soga, H. Nagayama, K. Hosoya, N. Tanaka, Anal. Chem. 72 (2000) 1275.
[34] A. Cavazzini, G. Bardin, K. Kaczmarski, P. Szabelski, M. Al-Bokari, G. Guiochon, J. Chromatogr. A 957 (2002) 111.
[35] M. Al-Bokari, D. Cherrak, G. Guiochon, J. Chromatogr. A 975 (2002) 275.
[36] M. Motokawa, H. Kobayashi, N. Ishizuka, H. Minakuchi, K. Nakanishi, H. Jinnai, K. Hosoya, T. Ikegami, N. Tanaka, J. Chromatogr. A 961 (2002) 53.
[37] P. Flory, Principles of Polymer Chemistry, Cornell University Press, Ithaca, NY, 1971.
[38] K. Nakanishi, H. Shikata, N. Ishizuka, N. Koheiya, N. Soga, J. High Resolut. Chromatogr. 23 (2000) 106.
[39] C. Alié, R. Pirard, J.-P. Pirard, J. Non-Cryst. Solids 292 (2001) 138.
[40] E.P. Barrett, L.G. Joyner, P.P. Halenda, J. Am. Chem. Soc. 73 (1951) 373.
[41] S.J. Sing, K.S.W. Gregg, Adsorption Surface Area and Porosity, Academic Press, New York, 1982.